DISCRETE AND CONTINUOUS
DYNAMICAL SYSTEMS
Supplement 2009

Website: www.aimSciences.org

pp. **109–117**

MULTIPULSE STATES IN THE SWIFT-HOHENBERG EQUATION

J. Burke

Center for BioDynamics, Boston University, Boston, MA 02215, USA

E. Knobloch

Department of Physics, University of California, Berkeley, CA 94720, USA

Abstract. The one-dimensional Swift-Hohenberg equation is known to exhibit a variety of localized states within the so-called pinning or snaking region. Single-pulse states consist of single localized structures within the spatial domain, and are organized into a snakes-and-ladders structure within the pinning region. Multipulse states consist of two or more localized structures within the domain, but their detailed organization within the pinning region is not known. In this paper we consider multipulse solutions of the one-dimensional Swift-Hohenberg equation on large but periodic domains, and show that while these are also confined to the pinning region the details of their organization depend on whether the pulses are equidistant or not. For large domains the required branch-following becomes delicate and may lead to erroneous results unless performed with great care.

1. **Introduction.** The Swift-Hohenberg equation describes the formation of spatially periodic patterns with a finite wavenumber k_0 at onset. In one spatial dimension the equation takes the form

$$u_t = ru - \left(\partial_x^2 + k_0^2\right)^2 u + f(u)\,, \tag{1}$$

where $f(u)$ is a nonlinear term depending on u alone. This equation is variational and hence on periodic domains all solutions approach steady states. In the following we shall be interested in characterizing such states. The key to the properties of these states is provided by the equivariance of Eq. (1) with respect to the reversibility operator

$$R: \quad x \to -x, \quad u \to u\,, \tag{2}$$

as discussed in Refs. [6, 16]. On the real line this property is responsible for the presence of a reversible Hopf bifurcation with 1:1 resonance in the linear stability problem for the trivial solution $u = 0$ in *space*. Specifically, at $r = 0$ the (four) spatial eigenvalues are given by $\lambda = \pm ik_0$, each with double multiplicity. Moreover, for $r < 0$ these eigenvalues move off the imaginary axis and form a complex quartet $(\lambda = \pm(ik_0 \pm (\sqrt{-r}/2k_0)) + \mathcal{O}(r))$ while for $r > 0$ they also split but remain on the imaginary axis $(\lambda = \pm i(k_0 \pm (\sqrt{r}/2k_0) + \mathcal{O}(r)))$. The presence of this bifurcation can in turn be used to show that spatially periodic and spatially localized states biasymptotic to $u = 0$ bifurcate *simultaneously* from $u = 0$ as the bifurcation parameter r increases through $r = 0$ provided only that the former bifurcate

2000 *Mathematics Subject Classification.* Primary: 70K44, 37G15; Secondary: 37L15.
Key words and phrases. Localized states, Swift-Hohenberg equation, homoclinic snaking.

subcritically [5, 9]. The latter are of single-pulse form and undergo homoclinic snaking [5, 9, 12].

In this paper we consider the case $f(u) \equiv b_2u^2 - u^3$, which is the simplest nonlinearity that produces the bistability between the trivial and patterned states that is crucial in what follows. On the real line Eq. (1) can be scaled to eliminate k_0 so that the equation is fully parameterized by r and b_2. On a periodic domain with period Γ this is no longer the case, however, and we choose to retain k_0 to highlight the dependence of our results on the length scales $2\pi/k_0$ and Γ. For large Γ stationary, spatially periodic solutions with wavenumber k_0 set in at $r = 0$ and the resulting bifurcation is subcritical provided [5, 9]

$$q_2 \equiv \frac{3}{4k_0^2} - \frac{19b_2^2}{18k_0^6} < 0\,. \tag{3}$$

The resulting branch of spatially periodic states undergoes a saddle-node bifurcation at $|r| = \mathcal{O}(k_0^4)$, and hence at $\mathcal{O}(k_0^2)$ amplitude, whenever $q_2 = \mathcal{O}(k_0^{-2})$, as in Fig. 1.

On the real line, the localized states of interest approach $u = 0$ as $x \to \pm\infty$. When $q_2 < 0$ there are two branches of such states; both emerge subcritically from the trivial state $u = 0$ in a pitchfork bifurcation at $r = 0$. Near onset ($|r| \ll 1$) these states are weakly localized and are given by

$$u(x) = \frac{1}{k_0}\left(\frac{2r}{q_2}\right)^{1/2} \operatorname{sech}\left(\frac{x\sqrt{-r}}{2k_0}\right)\cos\left(k_0x + \phi\right) + \mathcal{O}(r)\,, \quad r < 0\,, \tag{4}$$

where $\phi = 0, \pi$ are the only values of the spatial phase ϕ for which expression (4) approximates true solutions of Eq. (1) [5]. We define L_0 and L_π as the branches of reflection-symmetric localized states found by continuing the approximation (4) with $\phi = 0, \pi$ to finite amplitude. Along L_0 the midpoint $x = 0$ of the localized state is a maximum, while along L_π it is a minimum. Both branches enter with decreasing r a region we refer to as the pinning or snaking region, $r_{P1} < r < r_{P2}$. In this region the localized states are strongly localized while their amplitude becomes comparable to that of the competing spatially periodic state. Within the snaking region each branch undergoes a series of back-and-forth oscillations (Fig. 1) as the localized structures grow by pairwise nucleation of spatial oscillations at either side, resulting in ever longer localized structures embedded in a background filled with the $u = 0$ state. The broad localized states found higher and higher up the two snaking branches are confined to the pinning region in r and are well approximated by *heteroclinic cycles* connecting the $u = 0$ state to the periodic state and back again. The wavenumber $k(r)$ of the pattern within these states varies across this region and is selected by the requirement

$$H \equiv -\frac{1}{2}(r - k_0^4)u^2 + k_0^2u_x^2 - \frac{1}{2}u_{xx}^2 + u_xu_{xxx} - \int_0^u f(v)dv \;= 0. \tag{5}$$

The resulting wavenumber range is characteristic of the localized states in the pinning region, and plays an important role in their behavior on a finite domain [3].

A more detailed analysis reveals that the branches L_0, L_π repeatedly gain and lose stability as one proceeds up the resulting snaking structure. In addition one finds that these branches are connected pairwise by secondary branches of *asymmetric* states forming a characteristic structure we call the snakes-and-ladders structure. These branches always connect unstable parts of the primary L_0, L_π branches (Fig. 1) although high up the snakes-and-ladders structure these secondary bifurcations approach closer and closer the saddle-node bifurcations.

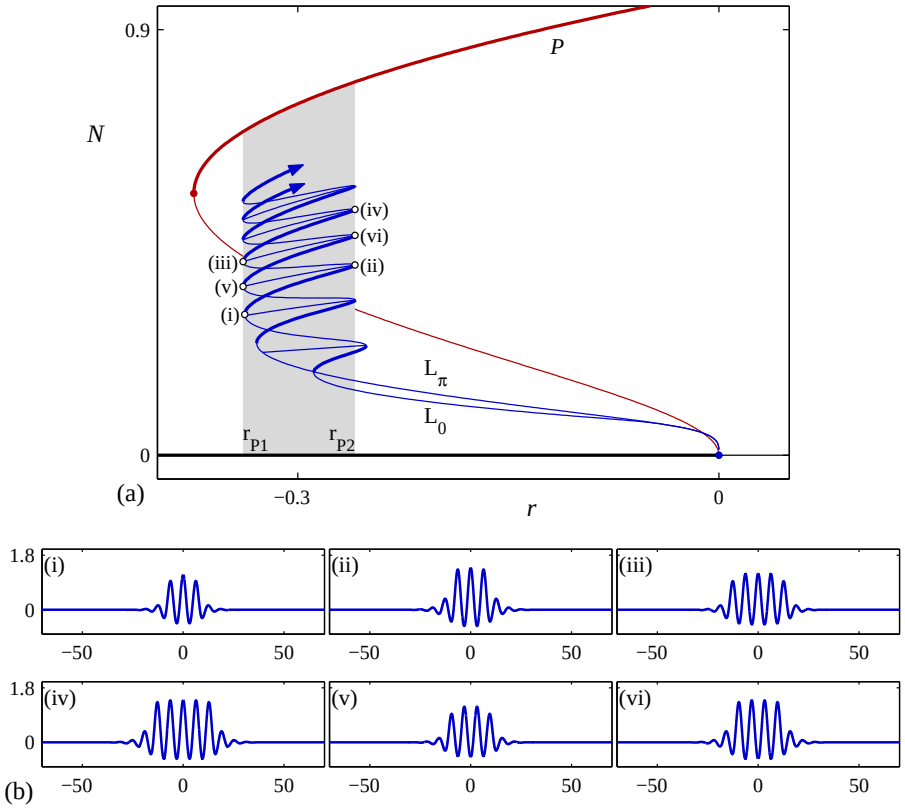

FIGURE 1. (a) Homoclinic snaking in Eq. (1) with $f(u) \equiv b_2 u^2 - u^3$. Stable (unstable) states are indicated by thick (thin) lines; N is the L^2 norm per unit length. The label P denotes spatially periodic states with wavenumber $k_0 = 1$. (b) Sample localized profiles $u(x)$. States (i)-(iv) are located at successive saddle-nodes on the L_0 branch; (v)-(vi) lie on L_π. Parameters: $k_0 = 1$, $b_2 = 1.8$.

In periodic domains of large but finite spatial period Γ the above scenario is necessarily modified [3]. One finds that the primary bifurcation to spatially periodic states breaks up into a succession of bifurcations to periodic solutions labeled P_n, where the integer n specifies the basic period Γ/n of the solutions along each branch. These bifurcate from the trivial state $u = 0$ when r reaches $r = r_n$, where

$$r_n = \left(k_0^2 - (2\pi n/\Gamma)^2\right)^2 > 0\,. \tag{6}$$

The single-pulse states L_0, L_π bifurcate together from the *first* of these spatially periodic branches in a secondary bifurcation, i.e., at finite amplitude. If Γ is large this secondary bifurcation takes place already at a very small amplitude. Moreover, since snaking cannot go on forever in finite domains, once the domain is filled with the localized state snaking must cease, and the branches L_0, L_π exit the pinning region and terminate on one of the branches of spatially periodic states $P_{n'}$. The termination branch may or may not be the same as the one from which the L_0, L_π branches bifurcate at small amplitude (i.e., n' may differ from the n that minimizes

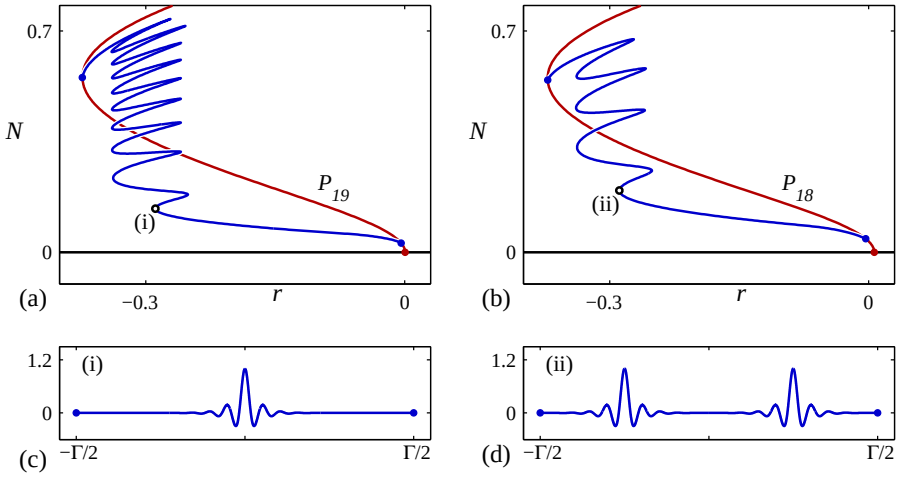

FIGURE 2. (a) Bifurcation diagrams showing the L_0 single-pulse snaking branch, which emerges from and terminates on the P_{19} spatially periodic branch. (b) Bifurcation diagram showing the branch of the two equidistant L_0 pulses on the same domain, which emerges from and terminates on P_{18}. (c,d) Sample profiles at the points indicated in the bifurcation diagrams. Parameters: $k_0 = 1$, $b_2 = 1.8$, $\Gamma = 118$.

r_n), and the two branches of localized states need not terminate together on the same spatially periodic branch. Roughly speaking, the termination branch is determined by the minimum wavenumber $k(r)$ selected by Eq. (5) within the pinning region, and its commensurability with the imposed period Γ. The termination point itself lies near the saddle-node on the termination branch, typically above it, although under some conditions (described in detail in [3]) it may fall below the saddle-node. Analogous results for finite domains with Dirichlet or Neumann boundary conditions are found in Ref. [7].

In the following we examine the corresponding results for multipulse states.

2. **Two-pulse states.** The Swift-Hohenberg equation possesses a large variety of multipulse solutions resembling a number of single-pulse states replicated within the spatial domain. Many such states are possible depending on the number of pulses included, the width of each pulse, and the separation between neighboring pulses. On the real line there is an infinite number of such states, while the number on bounded domains is finite. When the individual pulses are well separated one may think of these as "bound states" of single-pulse solutions interacting weakly via their overlapping tails. This type of analysis has been considered by a number of authors (see [1, 17] and references therein).

We present here a partial description of two-pulse solutions to (1) on a periodic domain of length Γ. We focus on time-independent solutions of the form $u(x) = u(-x)$, but in this case the profiles of interest contain two symmetrically related pulses, one in each half of the domain. The simplest class of such states consists of two identical pulses whose centers are separated by a distance $\Gamma/2$. Evidently, such pulses are equidistant from their nearest neighbors on either side, and hence their

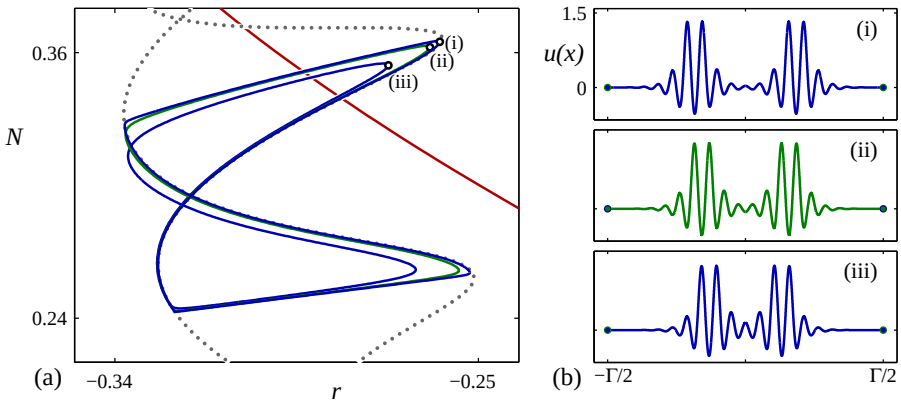

FIGURE 3. (a) Bifurcation diagram showing isolas of symmetric two-pulse states. The nested isolas correspond to fixed pulse width as the pulse separation varies. For reference, the snaking branches of equidistant two-pulse states are plotted as dotted lines. (b) Profiles at the points labeled in the bifurcation diagram. Parameters: $k_0 = 1$, $b_2 = 1.8$, $\Gamma = 118$.

behavior is identical to the behavior of single-pulse states on a periodic domain of length $\Gamma/2$. The solutions are therefore organized into a pair of snaking branches, one of which consists of two L_0 pulses while the other consists of two L_π pulses. Figure 2 compares the L_0 branches of single-pulse and equidistant two-pulse states in a domain with $\Gamma = 118$. As already mentioned the single-pulse snaking branches bifurcate together from the first spatially periodic branch that emerges in $r \geq 0$ [3, 5], here P_{19}. However, the equidistant two-pulse states must bifurcate from the first spatially periodic branch in $r \geq 0$ that includes an *even* number n of wavelengths in Γ. This branch may or may not be the same branch as that from which the single-pulse states emerge, and indeed in the example shown in Fig. 2(b) the two-pulse states bifurcate from P_{18}, i.e., a branch that bifurcates from $u = 0$ subsequent to the first spatially periodic branch P_{19}. Like the single-pulse states, the equidistant two-pulse states must terminate once the domain is filled, and this necessarily occurs on a branch of spatially periodic states that contains an even number n' of wavelengths in Γ. In the example shown in Fig. 2(b) the two-pulse states terminate on the same branch from which they originate, P_{18}. The behavior of the corresponding L_π states (not shown) is very similar.

We also find a large number of states consisting of two pulses per period related by reflection through a suitable origin, whose centers are *not* separated by $\Gamma/2$. The allowed separations are discrete as determined by the interaction between the oscillatory tails of the pulses. These unevenly spaced two-pulse states are organized into *isolas* and do not connect directly to the spatially periodic branches (Figs. 3 and 4). Each isola has a characteristic 'figure eight' structure, first identified in [14, 15], consisting of a segment where the individual pulses resemble L_0 profiles and a segment where they resemble L_π profiles, connected to one another by two segments where the individual pulses resemble the asymmetric profiles from the rungs of the snakes-and-ladders structure of the single-pulse states. In each case the pulses are slightly deformed from the single-pulse shapes due to their mutual interaction.

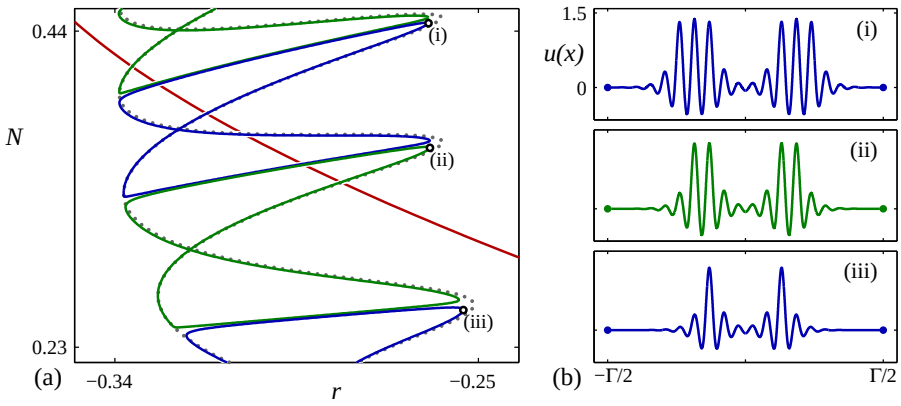

FIGURE 4. (a) Bifurcation diagram showing isolas of symmetric two-pulse states. The stack of isolas corresponds to fixed pulse separation as the individual pulse width grows. (b) Profiles at the points labeled in the bifurcation diagram. Parameters: $k_0 = 1$, $b_2 = 1.8$, $\Gamma = 118$.

Along each isola the separation between the pulses is (roughly) constant. At fixed pulse width the discrete number of allowed pulse separations creates a discrete family of nested isolas (Fig. 3). If one fixes instead the separation between the two pulses one finds that the discrete pulse widths create a family of stacked isolas (Fig. 4). The full bifurcation diagram for two-pulse states of this type therefore consists of a stack of nested isolas.

On large domains the difference between adjacent isolas in a stack becomes exponentially small, making it difficult to trace out numerically the isolas associated with pulses whose edges are separated by more than a few wavelengths $2\pi/k_0$. In Fig. 5 we show the results of continuation of two-pulse states with different accuracy: with inadequate accuracy the code has a difficult time continuing from the snake-like segment of an isola to the rung-like segment, and instead jumps branches near the saddle-node to the snake-like segment of the next isola in the stack. This occurs until the profiles are broad enough that the two pulses interact more strongly, resulting in a rung-like segment that can be followed more easily. At this point the continuation code is able to traverse the bifurcation diagram from the L_0 branch, say, to the L_π branch (or vice versa) thereby truncating the snakes-and-ladders structure. Diagrams of this type can be found, for example, in [11, 15].

There are many more two-pulse states where the individual pulses are not related by reflection in x. Most of these are organized in branches which do not connect directly to the spatially periodic branches, and instead form isolas (similar to those described above) or secondary branches which bifurcate from the isolas. However, there is a branch of non-symmetric two-pulse states which emerges directly from the first spatially periodic branch in $r \geq 0$ that includes an *odd* number n of wavelengths in Γ (Fig. 6). The solutions along this branch resemble a bound state of a $\phi = 0$ profile and a $\phi = \pi$ profile whose centers are separated by $\Gamma/2$. The two pulses alternately nucleate pairs of additional peaks as one moves up the branch, thereby tracing out segments on the bifurcation diagram which resemble each of the two snaking branches connected by segments which resemble the rungs.

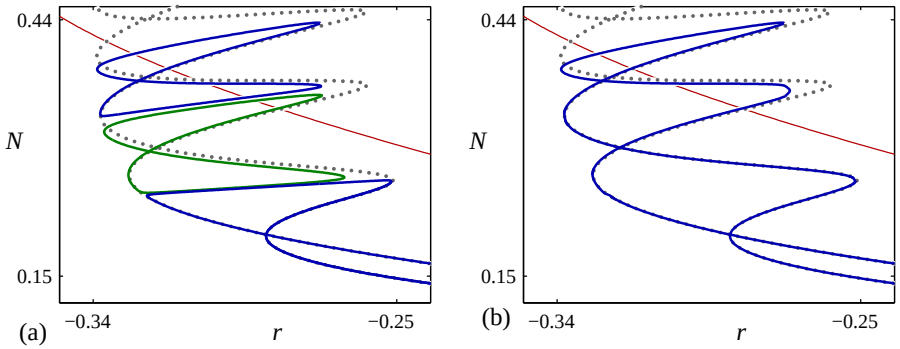

FIGURE 5. (a) Bifurcation diagram showing a stack of three isolas of two-pulse localized states. (b) Bifurcation diagram traced out using insufficient accuracy. The numerical branch-following routine "jumps" between the actual branches, tracing out one large isola. Parameters: $k_0 = 1$, $b_2 = 1.8$, $\Gamma = 118$.

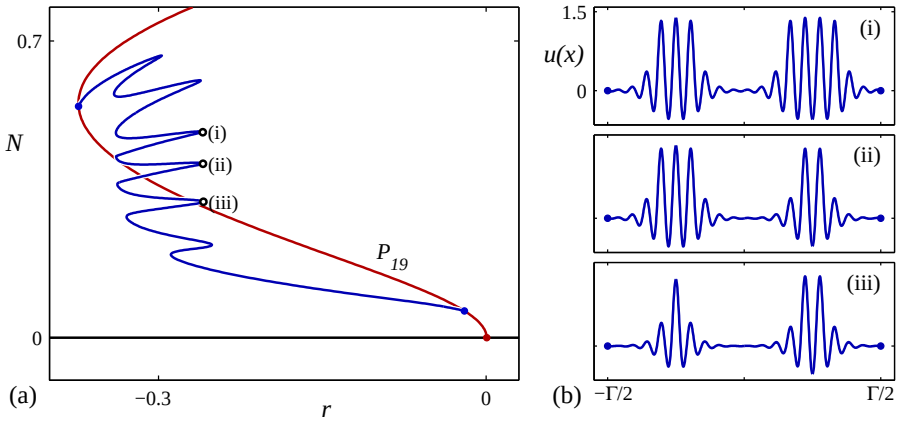

FIGURE 6. (a) Bifurcation diagram showing a branch of non-symmetric two-pulse localized states which emerges from and terminates on the spatially periodic branch P_{19}. (b) Profiles at the points labeled in the bifurcation diagram. Parameters: $k_0 = 1$, $b_2 = 1.8$, $\Gamma = 118$.

3. **Conclusions.** In this note we have shown that two-pulse localized solutions of the Swift-Hohenberg equation on large periodic domains either snake (if the resulting pulses are equidistant) or are located on figure-eight-like isolas. The latter are organized in a vertical stack that can be viewed as the result of a breakup of the single-pulse snakes-and-ladders structure due to interpulse interaction. Stability with respect to amplitude perturbations is inherited from the underlying snakes-and-ladders structure in the obvious fashion: two-pulse states on the portion of the figure-eight between the lower left saddle-node and the upper right saddle-node are stable, and all others are unstable. All isolas come in nested families depending on the width of the two pulses, and all stacks of such nested isolas coexist

simultaneously with the snaking structure of the equidistant two-pulse states. We expect that the techniques recently introduced by Beck et al. [2] can be extended to multipulse states and used to explain why such states are generically found on isolas as opposed to snaking branches.

As we have seen the details of the predicted behavior depend crucially on whether the spatial domain is the whole real line or a periodic domain of finite spatial period. In the latter the two single-pulse snaking branches may terminate on different branches of periodic states. Since the termination points are secondary pitchfork bifurcations it follows that in these cases there are other branches that must terminate at these termination points. These correspond to so-called *Mixed Modes* and do not snake [3]. Additional changes occur in bounded domains with non-Neumann boundary conditions [8].

We mention that figure-eight-like isolas are a common feature of problems of this type and are found not only in the break-up of homoclinic snaking between two homogeneous states [5], but also in the break-up of homoclinic snaking due to forced breaking of spatial reversibility [4]. They are also present in problems involving the break-up of resonances, both temporal [10] and spatial [13].

The presence of multipulse states adds immeasurably to an already complex picture of the pinning region. Since many of the states in this region are stable large amplitude random initial conditions in this region lead to evolution of the system that is essentially unpredictable.

Acknowledgments. This work was supported by the National Science Foundation under grant DMS-0605238. We are indebted to S. Houghton and T. Wagenknecht for helpful discussions.

REFERENCES

[1] N. J. Balmforth, *Solitary waves and homoclinic orbits*, Ann. Rev. Fluid Mech., **27** (1995), 335–373.
[2] M. Beck, J. Knobloch, D. Lloyd, B. Sandstede, and T. Wagenknecht, *Snakes, ladders, and isolas of localised patterns*, SIAM J. Math. Anal., **41** (2009), 936–972.
[3] A. Bergeon, J. Burke, E. Knobloch, and I. Mercader, *Eckhaus instability and homoclinic snaking*, Phys. Rev. E, **78** (2008), 046201 (16pp).
[4] J. Burke, S. Houghton, and E. Knobloch, *Swift-Hohenberg equation with broken reflection symmetry*, Phys. Rev. E, in press.
[5] J. Burke and E. Knobloch, *Localized states in the generalized Swift-Hohenberg equation*, Phys. Rev. E, **73** (2006), 056211 (15pp).
[6] P. Coullet, C. Riera, and C. Tresser, *Stable static localized structures in one dimension*, Phys. Rev. Lett., **84** (2000), 3069 (4pp).
[7] J. H. P. Dawes, *Modulated and localised states in a finite domain*, SIAM J. Appl. Dyn. Syst., **8** (2009), 909–930.
[8] S. M. Houghton and E. Knobloch, *Homoclinic snaking in bounded domains*,. Phys. Rev. E, in press.
[9] G. W. Hunt, M. A. Peletier, A. R. Champneys, P. D. Woods, M. Ahmer Wadee, C. J. Budd, and G. J. Lord, *Cellular buckling in long structures*, Nonlinear Dynamics, **21** (2000), 3–29.
[10] V. Kirk, *Merging of resonance tongues*, Physica D, **66** (1993), 267–281.
[11] J. Knobloch and T. Wagenknecht, *Snaking of multiple homoclinic orbits in reversible systems*, SIAM J. Appl. Dyn. Syst., **7** (2008), 1397–1420.
[12] G. Kozyreff and S. J. Chapman, *Asymptotics of large bound states of localized structures*, Phys. Rev. Lett., **97** (2006), 044502 (4pp).
[13] J. Porter and E. Knobloch, *Complex dynamics in the 1:3 spatial resonance*, Physica D, **143** (2000), 138–168.

[14] G. H. M. van der Heijden, A. R. Champneys, and J. M. T. Thompson, *Spatially complex localisation in twisted elastic rods constrained to a cylinder*, Int. J. Solids and Structures, **39** (2002), 1863–1883.
[15] M. K. Wadee, C. D. Coman, and A. P. Bassom, *Solitary wave interaction phenomena in a strut buckling model incorporating restabilisation*, Physica D, **163** (2002), 26–48.
[16] P. D. Woods and A. R. Champneys, *Heteroclinic tangles and homoclinic snaking in the unfolding of a degenerate reversible Hamiltonian-Hopf bifurcation*, Physica D, **129** (1999), 147–170.
[17] S. Zelik and A. Mielke, *Multi-pulse evolution and space-time chaos in dissipative systems*, Mem. Amer. Math. Soc., **198** (2009), 1–97.

Received September 2008; revised March 2009.

E-mail address: jb@math.bu.edu
E-mail address: knobloch@px1.berkeley.edu